INTERNATIONAL JOURNAL OF CLIMATOLOGY
Int. J. Climatol. **34**: 1385–1394 (2014)
Published online 22 June 2013 in Wiley Online Library
(wileyonlinelibrary.com) DOI: 10.1002/joc.3767

RMetS
Royal Meteorological Society

Associations between circulation pattern frequencies and sea ice minima in the western Arctic

Thomas J. Ballinger* and Scott C. Sheridan

Department of Geography, Kent State University, Kent, OH, USA

ABSTRACT: In this study, a synoptic climatological approach is employed to assess the relationship between the frequency of circulation patterns (CPs) and the latitude of mid-September sea ice minima in the western Arctic. Fifteen CPs are created via principal component analysis and cluster analysis from daily NCEP/NCAR reanalysis sea-level pressure (SLP) fields across a grid from 50 to 90°N and 150°E–100°W from 1979 to 2011. The frequency of these CPs are statistically compared with the latitude of the sea ice minimum from passive microwave data for each of 11 equally-spaced longitudes (176°W to 126°W) extending into the Chukchi and Beaufort Seas. Monthly frequencies for each of the 15 CPs from March to September, signifying the melt season, for each year are correlated with the ice minimum for that September. These monthly frequencies are then entered into a stepwise multiple linear regression (SMLR) and collectively, CP frequencies explain 40–79% of the total ice retreat variance across the longitudes. The frequency of one cluster, CP 11, representing a broad high pressure area over the Beaufort Sea, is highly correlated with the latitude of the sea ice minima; June and August frequencies of this pattern are the initial predictors at 8 of the 11 longitudes and explain 22–32% of the variance. This pattern has occurred more frequently from 2007 onwards; compared with a June mean occurrence of 9 days during 1979–2006, CP 11 occurred 16 times in June 2007, and on average more than 17 days per month during June 2008–2011. The Arctic Dipole (AD), Arctic Oscillation (AO), and Pacific-North American (PNA) pattern indices are significantly correlated with CPs 11–13 frequencies throughout certain summer months, further indicating strong relationships between summer circulation and sea ice minima in the region.

KEY WORDS synoptic climatology; western Arctic; sea ice; circulation patterns; teleconnections

Received 29 October 2012; Revised 10 May 2013; Accepted 19 May 2013

1. Introduction

September Arctic sea ice extent has decreased nearly 12% dec^{-1} since 1979 (Stroeve *et al.*, 2012) with the largest extent losses occurring in the western Arctic, including the Beaufort and Chukchi Seas (Perovich and Richter-Menge, 2009). This region's summer sea ice losses in the 1990s (Maslanik *et al.* 1996; 1999) and 2000s (Stroeve *et al.*, 2005; Maslanik *et al.*, 2007b) have largely fueled the recurring Arctic-wide record minima over the last two decades. During this time thick, multi-year ice (MYI) has dramatically declined in the Beaufort Sea and Canada Basin (Kwok and Cunningham, 2010; Maslanik *et al.*, 2011; Derksen *et al.*, 2012) amidst a transition to thin, fragile first-year, or seasonal, ice cover that has also rapidly dissipated (Barber *et al.*, 2012). Several interconnected factors have potentially contributed to recently observed changes to the summer ice cover in the region including the ice-albedo feedback (e.g. Lindsay and Zhang, 2005), oceanic heat flux from the Pacific Ocean (e.g. Woodgate *et al.*, 2010), solar heating of the open ocean (e.g. Perovich *et al.*, 2007), and aspects of regional atmospheric circulation (e.g. Ogi and Wallace, 2012).

Synoptic circulation patterns (CPs) occurring throughout the melt season (from the March maximum to September minimum in the Northern Hemisphere) have been directly connected to western Arctic ice extent behaviour during summer. Though high pressure over this region is typically stronger and broader due to enhanced baroclinity in winter and spring (Serreze and Barrett, 2011), summer anticyclone activity is arguably more important in directly dictating summer loss. A strong Beaufort High during summer promotes ice loss due to warm air advection (Rogers, 1978) and increases ice export out of the region (Drobot and Maslanik, 2003). In recent years, this pattern has been especially pronounced in conjunction with record ice extent losses. For instance, Ogi *et al.* (2008) found mean summer (JAS) sea-level pressure (SLP) over the Beaufort Sea in 2007 to be higher than during any summer since 1979. The persistence of this synoptic setting permitted a reduction in western Arctic cloudiness (Kay *et al.*, 2008) and strong solar heating of the ocean which propelled the anomalous melt that transpired (Perovich *et al.*, 2008).

Cyclonic activity also has an important bearing on the summer ice edge. Climatologies of broad-scale low pressure activity in the Arctic indicate that frequency typically increases through spring and peaks in summer (Serreze *et al.*, 1993). Simmonds and Keay (2009) indicated that

* Correspondence to: T. J. Ballinger, Department of Geography, Kent State University, Kent, OH, USA. E-mail: tballin1@kent.edu

strength, as opposed to frequency, of recent migratory summer storms across the Arctic basin has substantially contributed to the negative September ice cover trend. Case studies by Asplin *et al.* (2012) and Parkinson and Comiso (2013) showed that strong winds and large waves from cyclones passing over open western Arctic waters in early September 2009 and August 2013, respectively, aided in the breakup of an already retreating ice edge.

In connection with synoptic patterns, atmospheric and oceanic teleconnections also have multifaceted and temporally varying associations with ice in the region. The Arctic Dipole (AD) has been linked to strong meridional wind forcing and export of sea ice out of the Beaufort basin during recent high loss summers (Wang *et al.*, 2009; Overland and Wang, 2010). The Pacific-North American (PNA) pattern was three standard deviations above its mean during summer 2007 with a pronounced 500 hPa ridge over the western Arctic (L'Heureux *et al.*, 2008). Rigor and Wallace (2004) found the negative phase of the summer Arctic Oscillation (AO) was associated with low sea ice concentrations in the Beaufort and Chukchi Seas due to warm air advection off the adjacent land and southerly, wind-driven transport of ice out of the region. The Pacific Decadal Oscillation (PDO), which has been mostly in positive phase since the mid-1970s, has also been associated with changes in Pacific sector sea ice and western Arctic surface air temperature in recent decades (Hartmann and Wendler, 2005; Danielson *et al.*, 2011).

Studies of regional atmospheric circulation and teleconnections over the Arctic Ocean often focus on one or two pressure features that have pronounced climatic impacts. Rather than focus solely on distinct spatial and temporal characteristics of specified semi-permanent pressure features, synoptic climatology provides an opportunity to identify a range of weather conditions related to the surface environment (Yarnal, 1993). There are two distinct synoptic classification realms: weather typing, which characterizes surface weather conditions, and circulation pattern (CP) identification, which partitions a single atmospheric level into common synoptic-scale flow regimes (Yarnal, 1993). In the western Arctic, weather typing (e.g. Kalkstein *et al.*, 1990) and hybrid approaches that integrate both classification schemes (e.g. Mülmenstädt *et al.*, 2012) have been seldom used. Circulation pattern classifications have been mainly used to evaluate surface circulation (i.e. SLP) effects on local temperature, precipitation, and wind regimes in the region (e.g. Cassano *et al.*, 2006; Cassano and Cassano, 2010; Cassano *et al.*, 2011). Few studies have examined relationships between atmospheric CPs and sea ice (e.g. Maslanik *et al.*, 2007a; Asplin *et al.*, 2009; Higgins and Cassano, 2009).

The purpose of this article is to create a synoptic circulation classification for the western Arctic in order to depict the array of SLP patterns that may play a role in the mid-September sea ice minimum in the Beaufort and Chukchi Seas. Aside from creating a holistic representation of SLP patterns over the region, this study focuses on the frequency of these events over the course of the melt season and their statistical relationships to the sea ice over time. Statistically significant relationships between monthly CPs and ice across multiple longitudes are further examined in the context of recent years, during which record loss of sea ice has been observed. Relationships between CPs and teleconnections known to impact western Arctic ice are also explored. This article is divided up as follows: Section 2 presents the data and methodology in detail. Section 3 covers the results including an introduction of the synoptic patterns, statistical connections to the ice, interannual variability/evolution of select patterns, and CP relationships to atmospheric and oceanic circulation teleconnections also relevant to western Arctic climate. Section 4 provides a discussion of the main findings. Section 5 briefly summarizes the results and discusses the potential for synoptic climatological applications in further assessing sea ice–climate interactions in the Arctic.

2. Data and methodology

2.1. Data

Reanalysis datasets are particularly useful over the polar regions in part because weather stations in these areas are sparsely configured and typically have short temporal resolutions. In this study, we use daily mean SLP data from the NCEP/NCAR reanalysis (Kalnay *et al.*, 1996) on a $2.5^\circ \times 2.5^\circ$ latitude/longitude grid (a total of 765 points) across the domain of 50–90°N and 150°E–100°W (Figure 1) from 1979 to 2011 to capture the SLP patterns associated with the Chukchi and Beaufort sea ice minimum in mid-September. SLP is utilized in this study because it can be used to indicate a number of different surface conditions including wind speed, wind direction, cloud cover and sunlight over an area, all of which play a vital role in modulating the ice cover. NCEP/NCAR circulation fields, SLP and otherwise, have been evaluated extensively in the Arctic and are known to produce comparable results to other reanalyses over the region (e.g. Serreze *et al.*, 2009; Cassano *et al.*, 2011; Serreze and Barrett, 2011). This data is obtained from NOAA/ESRL Physical Sciences Division.

Sea ice edge data for mid-September, which is the approximate climatological minimum (Comiso, 2002), are obtained from two different passive microwave datasets, HadISST and AMSR-E. Hadley Center Sea Ice and Sea Surface Temperatures (HadISST) monthly median sea ice concentration fields on a $1^\circ \times 1^\circ$ grid, 1979–2007, are from the Met Office Hadley Center (Rayner *et al.*, 2003). The sea ice edge from 2008 to 2011 is from the Advanced Microwave Scanning Radiometer-EOS (AMSR-E) archive available at the University of Bremen. The AMSR-E sea ice charts date back to 2003 and these data are well correlated with the HadISST-derived ice edge for overlapping years 2003–2007 ($r = +0.96$ to $+0.99$ depending on the longitude). Ice extent for mid-September, in terms of latitudinal retreat, is found in both datasets using the 50%

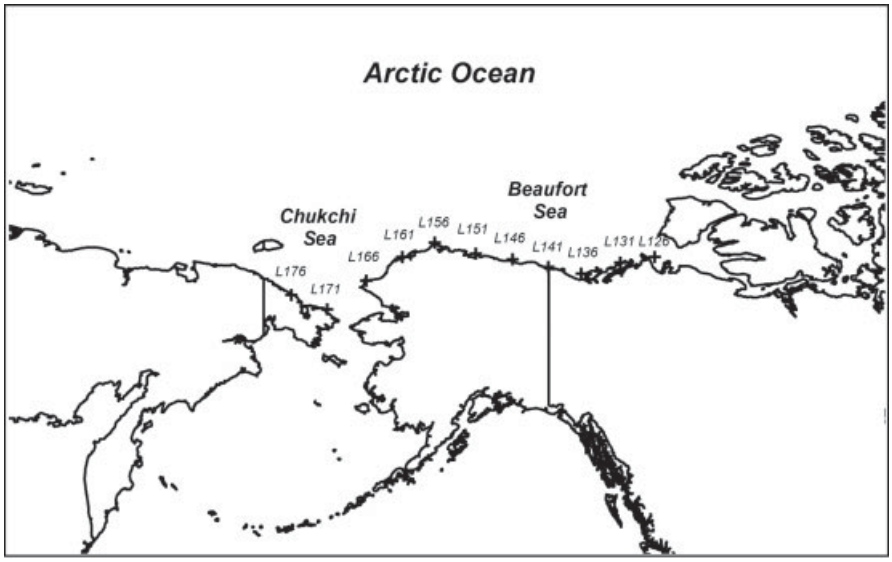

Figure 1. Map of the western Arctic domain. The 11 longitudes from which the latitude of the mid-September sea ice retreat is measured are indicated.

ice concentration threshold along 11 longitudes extending from the Alaskan and Siberian coasts into the Chukchi and Beaufort Seas (Figure 1). These longitudes are located at equally-spaced 5° intervals from 176°W (hereafter L176) in the eastern Chukchi Sea to 126°W (L126) in the eastern Beaufort Sea. The latitude of the ice edge is determined at sea unless the sea ice is fast to the coastline, in which case the extent is equal to the coastal latitude along the given longitude.

Four monthly atmospheric/oceanic teleconnection indices are also assessed in relation to the ice extent minimum. The Pacific-North American (PNA) pattern (Wallace and Gutzler, 1981) is one of the leading modes of Northern Hemisphere atmospheric variability and is created using a rotated principal component analysis (RPCA) technique on monthly mean 500 hPa height anomalies poleward of 20°N. Similar to Thompson and Wallace (1998), the AO is constructed by projecting the daily 1000 hPa height anomalies poleward of 20–90°N onto the loading pattern of the AO. The AO and PNA indices are obtained from the Climate Prediction Center (CPC). The AD is defined as the second Empirical Orthogonal Function (EOF) of the extended winter (NDJFM) mean SLP anomaly north of 70°N (Wang *et al.*, 2009; Overland and Wang, 2010), and were provided by James Overland and Muyin Wang. The PDO is the leading principal component of monthly SST poleward of 20°N (Mantua *et al.*, 1997) and these data are available from the Joint Institute for the Study of Atmosphere and Ocean (JISAO) at the University of Washington.

2.2. Methodology

The synoptic climatological classification used in this research involves a two-step synoptic climatological method employing both principal component analysis (PCA), which serves to reduce multicollinearity in the data set (Wilks, 2011), and cluster analysis, in which different SLP pattern types are created (Yarnal, 1993). Daily SLP values for each of the 765 grid points are entered into an S-mode PCA without any seasonal adjustments, as it is desired to identify interseasonal variability in the identified patterns. From the 765 data points, 26 principal components meet the generally accepted threshold for retention (an eigenvalue of at least 1), explaining 98.2% of the total SLP dataset variability over the specified domain.

These 26 retained principal components are then entered into a two-step cluster (TSC) technique, which classifies each day's spatial SLP features into an appropriate cluster. The primary goal of cluster analysis is to minimize variability within each cluster while maximizing the variability between clusters, though some within cluster variability must be assumed (Yarnal, 1993). Spekat *et al.* (2010) has suggested saving roughly 10–15 clusters for 30 years of daily data. When seasonality is not removed, there is a tendency for a greater number of winter-dominant clusters than summer-dominant ones, therefore the decision was made to save 15 clusters in order to better distinguish among summer CPs in particular, especially since relationships between end-of-summer sea ice extent and melt season-dominant patterns are the focus of this article. These patterns are created in SPSS using the log-likelihood distance measure and Schwarz's Bayesian information clustering criterion metrics (see Coleman and Rogers, 2007 for more TSC details).

Pearson's bivariate correlations between annual sea ice minima at each longitude and monthly CP frequencies that precede it are evaluated in detail. Correlations are only calculated for CPs whose mean monthly frequency exceeds 5% of days in months preceding the minima for a particular melt season (March to September; more description in Section 3.1.). In all, 47 total months across the 15 clusters met this frequency threshold. The monthly

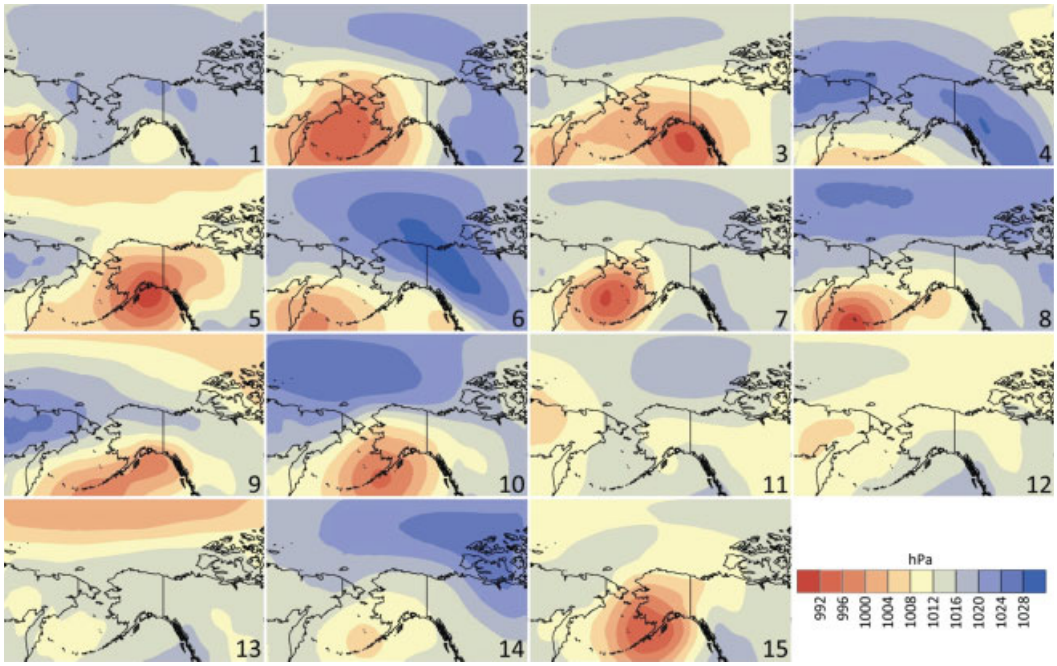

Figure 2. The 15 SLP circulation patterns generated from NCEP/NCAR reanalysis.

Table 1. Monthly frequencies (%) of the 15 circulation patterns from 1979 to 2011. The season in which they occur most frequently, winter (Wi), spring (Sp), summer (Su), and autumn (Au) are indicated in the final row.

Season	Month	**1**	**2**	**3**	**4**	**5**	**6**	**7**	**8**	**9**	**10**	**11**	**12**	**13**	**14**	**15**
Winter	January	7	13	8	11	7	13	5	6	17	6	<1	<1	<1	1	4
	February	8	13	7	11	7	11	4	9	14	8	<1	1	1	1	4
	March	8	6	7	6	6	10	6	11	8	13	1	2	2	5	7
Spring	April	6	3	5	4	4	2	9	15	2	15	5	3	5	17	5
	May	2	1	2	1	1	1	4	9	1	13	17	12	11	22	4
	June	1	<1	<1	<1	<1	<1	1	1	<1	2	34	25	25	10	1
Summer	July	<1	<1	<1	<1	<1	<1	1	1	<1	1	32	35	27	2	1
	August	1	1	1	1	1	<1	5	1	1	2	20	31	30	3	4
	September	5	4	3	2	6	1	10	3	3	6	12	13	15	6	13
Autumn	October	13	7	11	3	11	2	8	5	5	8	3	2	4	4	13
	November	16	12	14	4	8	7	10	4	8	7	<1	1	1	1	9
	December	8	13	14	10	9	10	7	5	11	6	<1	0	<1	1	4
		Au	Au/Wi	Au	Wi	Au	Wi	Au	Wi	Wi	Sp	Su	Su	Su	Sp	Au

CP frequencies are also introduced into a stepwise multiple linear regression (SMLR) model in order to evaluate their ability to hindcast mid-September sea ice extent along the 11 longitudes. SMLR involves a forward selection process whereby the initial predictor (CP frequency) explains the most predictand (sea ice) variance while subsequent predictors retained in the prediction equation must explain a significant amount of sea ice variance. All statistical results described are statistically significant at the 0.05 level unless noted otherwise.

3. Results

3.1. CP descriptions and relationships with sea ice

Due to the long seasonal lag evident in the Arctic, seasons are defined as follows: winter (JFM), spring (AMJ), summer (JAS), and autumn (OND). The 15 CPs are presented in Figure 2 and their monthly frequencies in Table 1. Patterns occurring more often from late winter (March) through the end of summer (September) are examined in greater detail as they occur during the melt season for each calendar year.

CPs 4, 6, 8, and 9 primarily occur during winter and exhibit fairly strong pressure gradients with pronounced low pressure centres over the North Pacific and high pressure areas over adjacent northeastern Siberia, eastern Alaska, Yukon and Northwest Territories and western Arctic Ocean. CPs 10 and 14 frequently occur during spring while patterns 11–13 mainly transpire during summer. These have much weaker pressure gradients as expected with a decreased thermal gradient. Of the three summer-dominant patterns: CP 11 exhibits a dome of high pressure over the Beaufort Sea (~1017 hPa), CP

Table 2. Statistically significant correlations between September ice extent (along 11 longitudes from 176 to 126°W indicated at the top) and CP frequency from 1979 to 2011. Italicized values are significant at $\alpha = .05$ and bold values are significant at $\alpha = .01$. Positive and negative correlation coefficients are indicated by the appropriate sign after the corresponding month. CPs 2, 4, 5, 6, and 9 had no significant correlations during the melt season and were therefore omitted from the table.

CP	L176	L171	L166	L161	L156	L151	L146	L141	L136	L131	L126
1	*3*$^+$	*3*$^+$	*3*$^+$	*3*$^+$	*3*$^+$	*3*$^+$	**3**$^+$	*3*$^+$			
3								*3*$^+$	**3**$^+$	**3**$^+$	**3**$^+$
7					*4*$^+$	*4*$^+$	**4**$^+$	*4*$^+$	*4*$^+$	**4**$^+$	*4*$^+$
8								*4*$^-$			
10								*9*$^-$	*9*$^-$	*9*$^-$	*9*$^-$
11	**6**$^+$	**6**$^+$	**6**$^+$	**6**$^+$	**6**$^+$	**6**$^+$	**6**$^+$	**6**$^+$	**6**$^+$	*6*$^+$	*6*$^+$
	8$^+$	**8**$^+$	**8**$^+$	*8*$^+$	*8*$^+$	*8*$^+$	*8*$^+$	*8*$^+$			*8*$^+$
12											*5*$^-$
				6$^-$							
											7$^-$
13	*6*$^-$	*6*$^-$	*6*$^-$	**6**$^-$	**6**$^-$	**6**$^-$	**6**$^-$	**6**$^-$	*6*$^-$	*6*$^-$	*6*$^-$
	8$^-$	*8*$^-$	*8*$^-$								
14			*5*$^+$						**5**$^+$	**5**$^+$	**5**$^+$
15										*4*$^+$	

12 has a broad, weak area of low pressure over that area (~1007 hPa) with slightly higher pressure just north of the Chukchi Sea (~1014 hPa), and CP 13 features a latitudinal pressure gradient, with fairly low pressure over the pole (~1001 hPa) increasing equatorward.

Correlations between the longitudinal ice extent minima and monthly CP frequencies are displayed in Table 2. Certain spring and summer CPs show particularly consistent and statistically significant connections to the ice. Specifically, CP 11 June shows a statistically significant positive correlation to the ice minimum at all longitudes ($r = +0.42$ to $+0.59$) while CP 11 August also displays this relationship with the exception of L136 and L131. CP 13 June demonstrates a significant negative correlation across all longitudes ($r = -0.37$ to -0.49) while CP 13 August only displays this relationship at L176-L166. Overall, more monthly CP frequencies are correlated to the ice at the easternmost longitudes, near the Canadian Archipelago, versus those in the western part of the domain, though some of these have associations with autumn-dominant patterns.

Given a number of strong connections to the ice cover, it is of no surprise that the late spring/summer CPs themselves also display a high level of predictability regarding the ice extent. The SMLR results (not shown) from all aforementioned CP frequencies explain between 40% (L151) and 79% (L141) of the mid-September ice extent variance across all longitudes from 1979 to 2011, with the variance explained generally increasing eastward (Figure 3(a)–(c)). September minimum extent in the eastern Beaufort is clearly less variable than in the western Beaufort and Chukchi seas, which may explain part of the reason why circulation is a better predictor of ice extent in this area. Figure 3(a) (L176) and (b) (L151) shows large amounts of unexplained variance over the time series, especially in the initial 10 years of the time series when the regression model shows a positive bias and overpredicts the observed ice extent latitude by ~1–5°. During the last 5 years (2007–2011), there are large positive residuals from under prediction at L151, but surprisingly not at L176. The entire 33 years sea ice extent time series at L126 is well explained by circulation ($r^2 = 0.74$). In terms of individual patterns, CP 11 June and August are the initial predictors at 8 of the longitudes (L176–L141) accounting for between 22 and 32% of the explained variance.

3.2. Late spring/early summer CP evolution

Analysis in Section 3.1. reveals that late spring/summer patterns are particularly well related to the western Arctic ice extent minima from 1979 to 2011. An examination of recent years (since the dramatic decline of 2007) versus the climatology (1979–2006) is warranted in order to address the role certain patterns, especially in the months directly preceding the minimum, may be playing on recent, historic mid-September losses in the region. Figure 4 shows the monthly frequencies of CPs 11–13 for June, July and August over three temporal delineations, 1979–2006, 2007, and 2008–2011.

CP 11 occurred on roughly one-third of June days ($\mu = 9$ days mo^{-1}, $\sigma = 5.35$) from 1979 to 2006. However, during recent high ice loss years the June frequency of this pattern has increased and occurred on 16 occasions in 2007, which was 1.31σ above the 1979–2006 period mean, and transpired 17.3 times mo^{-1} on average from 2008 to 2011. Prior to 2007, CP 11 had only occurred more than 14 times during June on two occasions (1983 and 1997), however from 2007 to 2011 no June month experienced less than 15 days of CP 11. Increased persistence of CP 11 June coincided with declines in other summer patterns during that month, particularly CP 13 June whose occurrence decreased ~4 days mo^{-1} from 2007 to 2011 relative to the 1979–2006 average ($\mu = 8.1$ days mo^{-1}). CP 12 June frequency also declined from the (1979–2006) average during both 2007 (~2 days mo^{-1}) and 2008–2011 (~3 days mo^{-1}).

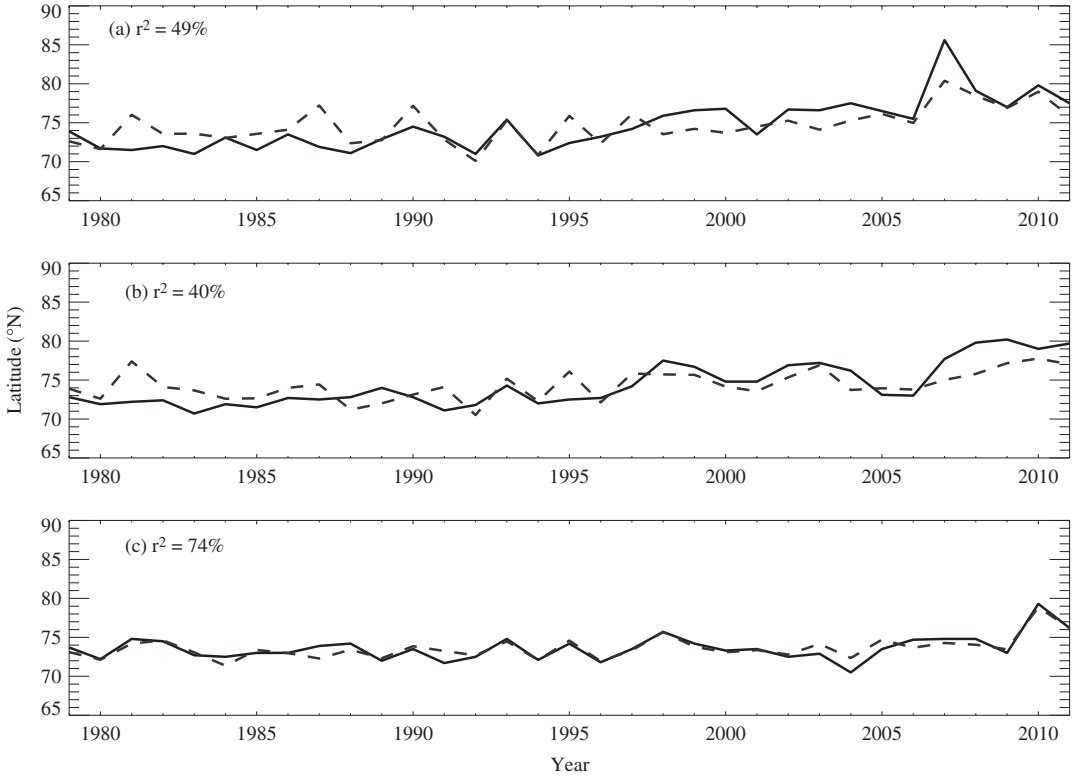

Figure 3. Observed sea ice retreat latitudes (solid) and predicted values (dashed) based on the SMLR equation for (a) L176, (b) L151, and (c) L126. Total explained sea ice extent variance (r^2) by the melt season synoptic patterns is indicated.

Though July frequencies for CPs 11–13 are minimally correlated with mid-September ice extent, their frequencies have changed substantially as well. During 2007, CP 11 July occurred 24 times or nearly 15 occasions more than the 1979–2006 average ($\mu = 9.1$ days mo^{-1}, $\sigma = 5.68$) and 2.62σ above the 1979–2006 mean. The CP 11 July pattern has continued to be more common in the recent period, occurring 11.5 days mo^{-1} from 2008 to 2011 at the expense of the summer-dominant patterns that were climatologically more common.

The evolution of August frequencies of CPs 11–13 is also worth noting. In 2007, CP 11 August occurred 18 times, which is nearly 13 more days than the extended August climatology ($\mu = 5.3$ days mo^{-1}, $\sigma = 3.7$) and 3.44σ above the long-term mean. It is worth noting that before 2007, CP 11 had only manifested more than 10 days in August during 2 years (1987 and 1990). From 2008 to 2011, the persistence of CP 11 August was 9.3 days mo^{-1}, still in excess of 4 days from the long-term mean. Similar to previous results, anomalous increases in CP 11 August frequencies are associated with CP 12 and 13 August decreases. As a result, CP 13 August frequency decreased by more than 2 days in 2007 (occurred only 7 days) and 2008–2011 ($\mu = 7.3$ days mo^{-1}) relative to the base period ($\mu = 9.8$ days mo^{-1}).

3.3. Relationships to teleconnections

As mentioned in Section 1, atmospheric and oceanic teleconnections have connections to the Arctic sea ice extent. In this section, monthly mean teleconnection indices are correlated to the monthly CPs frequencies (meeting the >5% threshold over the melt season) in an attempt to evaluate whether the western Arctic synoptic CPs are related to broader atmospheric and oceanic circulation influences. The correlations between CP frequency and the AD, AO, PNA pattern and PDO are presented in Table 3.

The AD is significantly correlated with many warm-season-dominant patterns. CP 11 frequencies are significantly negatively correlated with the AD index during June through August ($r = -0.58$ to -0.66), with a weaker correlation in September ($r = -0.37$). This suggests that increases (decreases) in the frequency of CP 11 follow decreases (increases) in the AD. To correspond with the CP11 relationship, the AD is positively correlated with both CP 12 and 13 in June ($r = +0.52$, $+0.61$) and July ($r = +0.58$, $+0.35$), which indicates that these pattern frequency increases (decreases) are tied to AD increases (decreases) during these months.

The AO and at least one CP are significantly correlated during all melt season months except August. In particular, CPs 11–14 June are significantly correlated with the AO during that month. CP 11 frequencies are negatively correlated with the AO during June ($r = -0.46$) and July ($r = -0.48$) indicating that an increase (decrease) in the frequency of CP 11 mirrors a decline (rise) in the AO 1000 hPa pressure centres. CP 13 frequencies are positively correlated with the AO during June ($r = +0.55$), July ($r = +0.57$), and September ($r = +0.64$), which indicates that pattern frequency increases (decreases) are

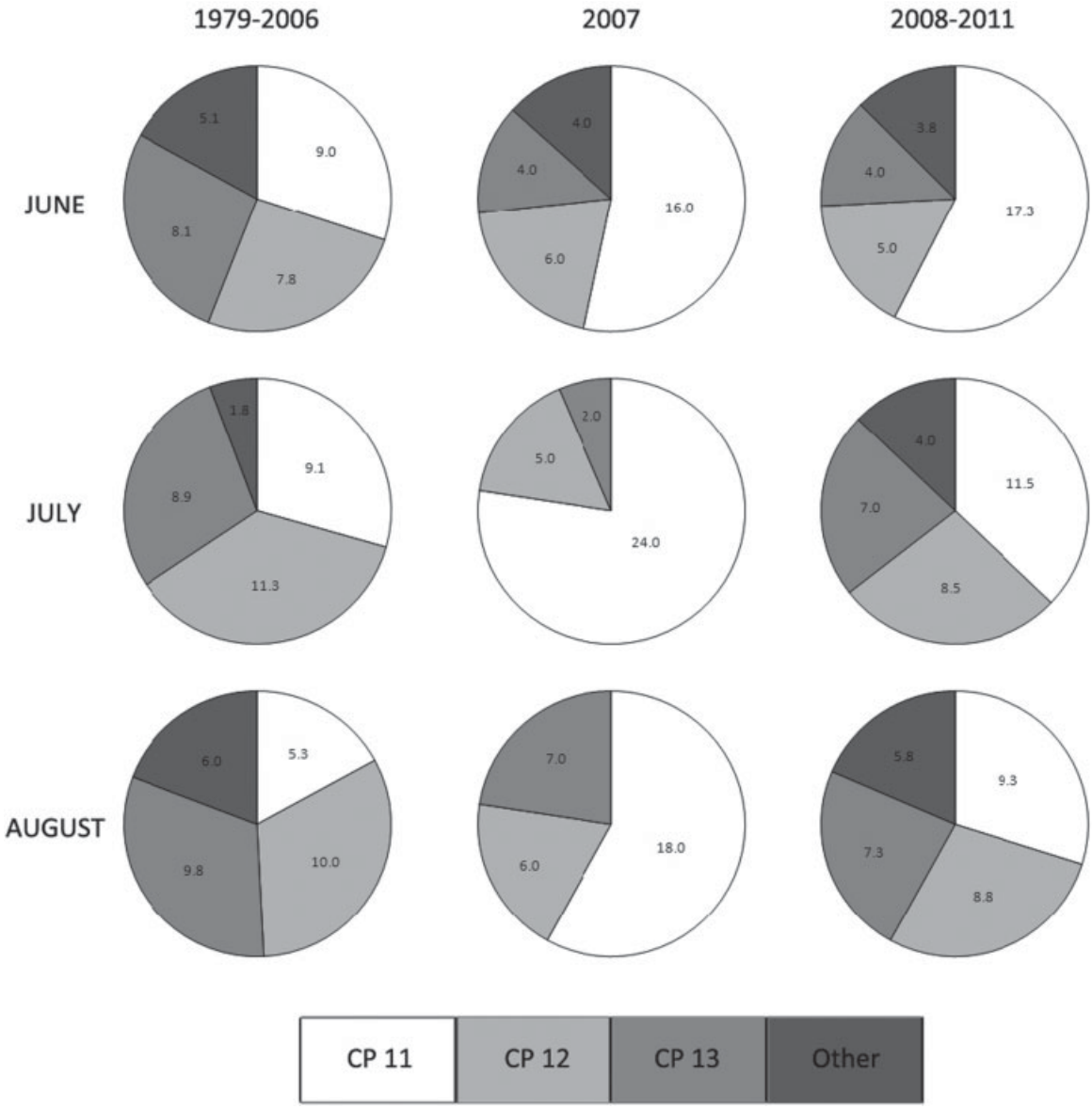

Figure 4. Pie charts indicating the frequencies of circulation patterns 11–13 over June, July, and August for 1979–2006, 2007, and 2008–2011. The number indicates the average occurrence for 1979–2006, 2008–2011, while the 2007 number indicates the occurrence for that year.

related to increases (decreases) in pressure anomalies affiliated with the teleconnection during summer.

While there were relatively few statistically significant PDO–CP correlations, including none after April, correlations between the CPs and the PNA revealed a large number of significant results. In late winter, CP 6 is significantly correlated with PNA in March. Despite its summer dominance, CP 10 is well correlated with the PNA in March and April. The positive correlation between CP 11 August and the August PNA index ($r = +0.62$) indicates that an increase (decrease) in the 500 hPa height field potentially increases (decreases) the frequency of CP 11. The negative correlation between CP 13 August ($r = -0.54$) and September ($r = -0.39$) and those months' PNA indices also indicates that an increase (decrease) in the PNA tends to decrease (increase) the frequency of CP 13 over the western Arctic.

4. Discussion

Whereas many studies have evaluated relationships between the summer sea ice edge and mean summer season circulation over the western Arctic, our study associates monthly CPs with the sea ice minimum and quantifies the number of days in which the patterns occurred in specified melt season months. Several CPs are statistically connected to the ice extent minimum measured across the 11 longitudes, most significantly the June and August frequencies of CP 11, and to a lesser extent CP 13. The frequency of CP 11, the Beaufort High, during late spring (June) and to a lesser extent mid-summer (August) is especially notable examining its temporal evolution in recent years. While CP 11 July and August frequencies well exceeded their respective 1979–2006 mean values in 2007 then decreased (Figure 4), CP 11 has been occurring more frequently in June since 2007. As previously

Table 3. Statistically significant correlations between monthly teleconnections (along 11 longitudes from 176 to 126°W indicated at the top) and CP frequency from 1979 to 2011. Italicized values are significant at $\alpha = .05$ and bold values are significant at $\alpha = .01$. Positive and negative correlation coefficients are indicated by the appropriate sign after the corresponding month. CPs 2, 4, and 15 have no significant correlations over the melt season.

CP	AD	AO	PDO	PNA
1		**4**$^{+}$	*4*$^{-}$	*4*$^{-}$
3			*4*$^{+}$	*4*$^{+}$
5				*9*$^{-}$
6				*3*$^{-}$
7				*3*$^{-}$
			3^{-}	*8*$^{-}$
				9^{-}
8		*3*$^{-}$	*4*$^{+}$	
		4^{+}		
		5^{-}		
9	*3*$^{+}$	**3**$^{+}$		
10		**3**$^{-}$		*3*$^{+}$
				4^{+}
11	**6**$^{-}$	*3*$^{+}$		**8**$^{+}$
	7^{-}	**6**$^{-}$		
	8^{-}	**7**$^{-}$		
	9^{-}			
12	**5**$^{+}$	**6**$^{+}$		*5*$^{-}$
	6^{+}			*7*$^{-}$
	7^{+}			
13	**6**$^{+}$	**6**$^{+}$	*4*$^{-}$	**8**$^{-}$
	7^{+}	**7**$^{+}$		*9*$^{-}$
		9^{+}		
14	**4**$^{-}$	**5**$^{-}$	*3*$^{+}$	*3*$^{+}$
	5^{-}	**6**$^{-}$		
	6^{-}	*9*$^{-}$		

indicated, past studies have highlighted the importance of this SLP feature during summer in conjunction with summer sea ice extent variability (e.g. Rogers, 1978; Drobot and Maslanik, 2003; Ogi *et al.*, 2008). It is important to note that as the thin, first-year ice cover has become more prevalent over time it has also become more susceptible to changes in atmospheric patterns (Stroeve *et al.*, 2012).

The increase in frequency of the Beaufort High since 2007 has coincided with a strengthening of its pressure field in recent years. Moore (2012) found that this anticyclone has strengthened at its climatological core during summers since the late 1990s and regional cyclogenesis has decreased due to tropospheric warming over the western Arctic. Ogi and Wallace (2012) indicated that 925 hPa circulation has become more anticyclonic in summers since 2007, though the 2010 and 2011 wind fields were not quite as strong as those experienced in 2007. The enhanced lower tropospheric flow promotes warm air advection on the western side of the anticyclone off the adjacent northern Alaskan land surface, thermodynamic thinning, and ice export across the Arctic Basin and toward the Fram Strait. Overland *et al.* (2012) observed a marked change in June meridional flow from 2007 to 2012 (versus previous decades) with a positive 700 hPa anomaly and corresponding pronounced MSLP field over the Beaufort Sea. The authors also suggest that these pressure anomalies over the western Arctic (i.e. the North American Ridge) are forcing the AD to persist and creating blocking patterns that are responsible for warming temperatures in parts of the Arctic, particularly downstream in Greenland. Our findings in Section 3.3. suggest that an increase in June-August Beaufort High frequency is directly related to a decrease in the AD (i.e. negative values) during those months, which is consistent with the findings of Overland *et al.* (2012).

Increased persistence of the Beaufort High since 2007 combined with its strengthening during late spring (June) and into summer (July, August) may partially explain why other common synoptic patterns have diminished in recent years and why dramatic end-of-summer ice loss has transpired in the Arctic, especially in the Beaufort and Chukchi Seas. High pressure anomalies (both in terms of strength and persistence) over the Beaufort Sea have triggered a number of observed events that are conducive to substantial sea ice thinning and melt. For instance, the 2007 persistence of the Beaufort High produced widespread clear skies and allowed substantial increases in solar heating of the upper ocean during the summer season (Perovich *et al.*, 2008), which manifested in SST anomalies of 0.5–2.5 °C during that summer (Steele *et al.*, 2008).

As stated in Section 1, the Beaufort High pressure signature is a staple in the winter and spring, but it is more centred and well-defined over the eastern Chukchi and Beaufort seas during the latter season as the pressure gradient weakens with changing seasonality and warmer temperatures (Serreze and Barrett, 2011). During summer, an even weaker surface pressure gradient is apparent and the Beaufort High shifts southward in the Beaufort and Chukchi Seas and includes northern Alaska and broadens to the east to cover the western Archipelago and northern Yukon, Northwest Territories, and Nunavut (Serreze and Barrett, 2011). A roughly similar spatial pattern is resolved by the synoptic technique employed in this study. It is important to remember that the Beaufort High resolved as CP 11 is an amalgamation of similar flow regimes over the course of a year, not just one season even though it is summer-dominant, so its strength will differ from climatological plots of seasonal fields. This pressure pattern is also a 'centre of action' for the AO and to a lesser extent the AD and PNA during summer (Serreze and Barrett, 2011), which is not surprising given the significant correlations identified in Section 3.3. and shown in Table 3.

Aside from a strong connection between CP 11 and the ice in particular, there is a noticeable spatial association as the number of CPs connected to western Arctic ice extent increases eastward across the longitudes. The resulting SMLR also shows an increasing amount of ice extent variance is explained by CPs in the eastern versus western half of the region. One reason why the westernmost ice variance (L176–L166) is relatively low ($r^2 \leq 0.49$ for each of the three longitudes) could be their proximity to the Pacific Ocean via the Bering Strait.

Warm water transfer from the Pacific into the western Arctic could be making substantial contributions to ice loss in recent years (Shimada *et al.*, 2006), especially in the Chukchi Sea (Woodgate *et al.*, 2010) where the westernmost ice longitude measurements of this study were derived. Aside from L151, the ice extent explained variance from L161 to L126 is 61% or higher (not shown). The higher variance and improved model fit of CPs to the ice extent data eastward toward the Canadian Arctic Archipelago indicates that circulation plays a larger role in explaining the mid-September ice extent in that part of the domain.

5. Conclusions

The synoptic CP classification performed in this study identified 15 SLP patterns typical over the specified western Arctic domain from 1979 to 2011, and correlated the frequencies of these patterns with sea ice extent as well as teleconnection indices. Certain late spring/summer patterns, especially CP 11 (which resolved the Beaufort High) and CP 13 are found to be well correlated to the September ice retreat. Both of these CPs are also well correlated with the AD and AO. The increasing frequency of CP 11 in June especially, but also during July and August, since 2007 has important consequences on the determining the extent of the ice retreat during the melt season, especially given continued thinning of the ice pack. Persistence of this anticyclonic feature corresponds to an enhanced wind field that promotes ice export out of the region while also yielding warm air advection off the land, clearing skies, positive solar radiation anomalies and coincident SST increases in the Beaufort/Chukchi region, which all perpetuate the ice-albedo feedback and stimulate further ice loss.

Aside from the limitations of the synoptic methodology outlined in Yarnal (1993), this study resolves a very concise spatial domain over the western Arctic. In doing so, other CPs that may have influence over the western Arctic ice cover may only be partially resolved or excluded entirely from the analysis. Future work that spatially expands both the ice and SLP fields across a larger Arctic domain may yield some interesting, comparative results over a similar time scale.

Future synoptic methodological studies of circulation over the region will be valuable to identify further connections between ice extent and regional circulation, especially with respect to time. One specific advantage of the synoptic climatological approach, as shown in this study, is that each day of the study period is categorized into one of several patterns which easily allows for the temporal progression of any pattern to be tracked. Arctic climate is expected to continue to warm through the 21st century in conjunction with persistent sea ice decline and anticipated changes in extreme SLP values during summer (Vavrus *et al.*, 2012). Identification of prominent monthly/seasonal CPs and their temporal evolutions moving forward will play a key role in understanding past summer losses and potentially predicting sea ice minima in the future.

Acknowledgements

The authors appreciate the helpful comments provided during the review process that improved this manuscript. The authors would also like to thank Meng-Pai Hung (NOAA/NWS/NCEP/Climate Prediction Center) for his programming assistance, Cameron Lee and Meg Petroski (Kent State University, Department of Geography) for their help plotting the circulation patterns, and James Overland (NOAA/PMEL) and Muyin Wang (JISAO/University of Washington) for sharing the AD data. TJB was supported by NSF Integrated Graduate Education and Research Training Grant DGE 0904560.

References

Asplin MG, Lukovich JV, Barber DG. 2009. Atmospheric forcing of the Beaufort Sea ice gyre: surface pressure climatology and sea ice motion. *Journal of Geophysical Research* **114**: C00A06. DOI: 10.1029/2008JC005127

Asplin MG, Galley R, Barber DG, Prinsenberg S. 2012. Fracture of summer perennial sea ice by ocean swell as a result of Arctic storms. *Journal of Geophysical Research* **117**: C06025. DOI: 10.1029/2011JC007221

Barber DG, Asplin MG, Papkryiakkou TN, Miller L, Else BGT, Iacozza J, Mundy CJ, Gosslin M, Asselin N, Ferguson S, Lukovich JV, Stern GA, Gaden A, Pućko M, Geilfus N-X, Wang F. 2012. Consequence of change and variability in sea ice on marine ecosystem and biogeochemical processes during the 2007–2008 Canadian International Polar Year program. *Climatic Change* **115**: 135–159.

Cassano EN, Cassano JJ. 2010. Synoptic forcing of precipitation in the Mackenzie and Yukon River basins. *International Journal of Climatology* **30**: 658–674.

Cassano EN, Lynch AH, Cassano JJ, Koslow MR. 2006. Classification of synoptic patterns in the western Arctic associated with extreme events at Barrow, Alaska, USA. *Climate Research* **30**: 83–97.

Cassano EN, Cassano JJ, Nolen M. 2011. Synoptic weather pattern controls on temperature in Alaska. *Journal of Geophysical Research* **116**: D11108. DOI: 10.1029/2010JD015341

Coleman JS, Rogers JC. 2007. A synoptic climatology of the central United States and associations with Pacific teleconnection pattern frequency. *Journal of Climate* **20**: 3485–3497.

Comiso JC. 2002. A rapidly declining perennial sea ice cover in the Arctic. *Geophysical Research Letters* **29**: 1956. DOI: 10.1029/2002GL015650

Danielson S, Curchitser E, Hedstrom K, Weingartner T, Stabeno P. 2011. On ocean and sea ice modes of variability in the Bering Sea. *Journal of Geophysical Research* **116**: C12034. DOI: 10.1029/2011JC007389

Derksen C, Smith SL, Sharp M, Brown L, Howell S, Copland L, Mueller DR, Gauthier Y, Fletcher CG, Tivy A, Bernier M, Bourgeois J, Brown R, Burn CR, Duguay C, Kushner P, Langlois A, Lewkowicz AG, Royer A, Walker A. 2012. Variability and change in the Canadian cryosphere. *Climatic Change* **115**: 59–88.

Drobot SD, Maslanik JA. 2003. Interannualvariability in summer Beaufort Sea ice conditions: relationship to winter and summer surface and atmospheric variability. *Journal of Geophysical Research* **108**: 3233. DOI: 10.1029/2002JC001537.

Hartmann B, Wendler G. 2005. The significance of the 1976 Pacific climate shift in the climatology of Alaska. *Journal of Climate* **18**: 4824–4839.

Higgins ME, Cassano JJ. 2009. Impacts of reduced sea ice on winter Arctic atmospheric circulation, precipitation, and temperature. *Journal of Geophysical Research* **114**: D16107. DOI: 10.1029/2009JD011884

Kalkstein LS, Dunne PC, Vose RS. 1990. Detection of climatic change in the western North American Arctic using a synoptic climatological approach. *Journal of Climate* **3**: 1153–1167.

Kalnay E, Kanamitsu M, Kistler R, Collins W, Deaven D, Gandin L, Iredell M, Saha S, White G, Woollen J, Zhu Y, Chelliah M, Ebisuzaki W, Higgins W, Janowiak J, Mo KC, Ropelewski C, Wang J, Leetmaa A, Reynolds R, Jenne R, Joseph D. 1996. The NCEP/NCAR 40-year reanalysis project. *Bulletin of the American Meteorological Society* **77**: 437–471.

Kay JE, L'Ecuyer T, Gettelman A, Stephens G, O'Dell C. 2008. The contribution of cloud and radiation anomalies to the 2007 Arctic sea ice extent minimum. *Geophysical Research Letters* **35**: L08503. DOI: 10.1029/2008GL033451

Kwok R, Cunningham GF. 2010. Contribution of melt in the Beaufort Sea to the decline in Arctic multiyear sea ice coverage: 1993–2009. *Geophysical Research Letters* **37**: L20501. DOI: 10.1029/2010GL044678

L'Heureux ML, Kumar A, Bell GD, Halpert MS, Higgins RW. 2008. Role of the Pacific-North American (PNA) pattern in 2007 Arctic sea ice decline. *Geophysical Research Letters* **35**: L20701. DOI: 10.1029/2008GL035205

Lindsay RW, Zhang J. 2005. The thinning of Arctic sea ice, 1988–2003: have we passed a tipping point? *Journal of Climate* **18**: 4879–4894.

Mantua NJ, Hare SR, Zhang Y, Wallace JM, Francis RC. 1997. A Pacific interdecadal climate oscillation with impacts on salmon production. *Bulletin of the American Meteorological Society* **78**: 1069–1079.

Maslanik JA, Serreze MC, Barry RG. 1996. Recent decreases in Arctic summer ice cover and linkages to atmospheric circulation anomalies. *Geophysical Research Letters* **23**: 1677–1680.

Maslanik JA, Serreze MC, Agnew T. 1999. On the record reduction in 1998 Western Arctic sea-ice cover. *Geophysical Research Letters* **26**: 1905–1908.

Maslanik J, Drobot S, Fowler C, Emery W, Barry R. 2007a. On the Arctic climate paradox and the continuing role of atmospheric circulation in affecting sea ice conditions. *Geophysical Research Letters* **34**: L03711. DOI: 10.1029/2006GL028269

Maslanik JA, Fowler C, Stroeve J, Drobot S, Zwally J, Yi D, Emery W. 2007b. A younger, thinner Arctic ice cover: increased potential for rapid extensive sea-ice loss. *Geophysical Research Letters* **34**: L24501. DOI: 10.1029/2007GL032043

Maslanik J, Stroeve J, Fowler C, Emery W. 2011. Distribution and trends in Arctic sea ice age through spring 2011. *Geophysical Research Letters* **38**: L13502. DOI: 10.1029/2011GL047735

Moore GWK. 2012. Decadal variability and a recent amplification of the summer Beaufort Sea High. *Geophysical Research Letters* **39**: L10807. DOI: 10.1029/2012GL051570

Mülmenstädt J, Lubin D, Russell LM, Vogelmann AM. 2012. Cloud properties over the North Slope of Alaska: identifying the prevailing meteorological regimes. *Journal of Climate* **25**: 8238–8258.

Ogi M, Wallace JM. 2012. The role of summer surface wind anomalies in summer Arctic sea ice extent in 2010 and 2011. *Geophysical Research Letters* **39**: L09704. DOI: 10.1029/2012GL051330

Ogi M, Rigor IG, McPhee MG, Wallace J. 2008. Summer retreat of Arctic sea ice: role of summer winds. *Geophysical Research Letters* **35**: L24701. DOI: 10.1029/2008GL035672

Overland JE, Wang M. 2010. Large-scale atmospheric circulation changes are associated with the recent loss of Arctic sea ice. *Tellus A* **62**: 1–9.

Overland JE, Francis JA, Hanna E, Wang M. 2012. The recent shift in early summer Arctic atmospheric circulation. *Geophysical Research Letters* **39**: L19804. DOI: 10.1029/2012GL053268

Parkinson CL, Comiso JC. 2013. On the 2012 record low Arctic sea ice cover: combined impact of preconditioning and an August storm. *Geophysical Research Letters* **40**: 1356–1361. DOI: 10.1002/grl.50349

Perovich DK, Richter-Menge JA. 2009. Loss of sea ice in the Arctic. *Annual Review of Marine Science* **1**: 417–441.

Perovich DK, Light B, Eicken H, Jones KF, Runciman K, Nghiem SV. 2007. Increasing solar heating of the Arctic Ocean and adjacent seas, 1979–2005: attribution and role in the ice-albedo feedback. *Geophysical Research Letters* **34**: L19505. DOI: 10.1029/2007GL031480

Perovich DK, Richter-Menge JA, Jones KF, Light B. 2008. Sunlight, water and ice: extreme Arctic sea ice melt during the summer of 2007. *Geophysical Research Letters* **35**: L11501. DOI: 10.1029/2008GL034007

Rayner NA, Parker DE, Horton EB, Folland CK, Alexander LV, Powell DP, Kent EC, Kaplan A. 2003. Global analysis of sea surface temperature, sea ice, and night marine air temperature since the late nineteenth century. *Journal of Geophysical Research* **108**: 4407. DOI: 10.1029/2002JD002670

Rigor IG, Wallace JM. 2004. Variations in the age of Arctic sea ice and summer sea-ice extent. *Geophysical Research Letters* **31**: L09401. DOI: 10.1029/2004GL019492

Rogers JC. 1978. Meteorological factors affecting interannual variability of summertime ice extent in the Beaufort Sea. *Monthly Weather Review* **106**: 890–897.

Serreze MC, Barrett AP. 2011. Characteristics of the Beaufort Sea high. *Journal of Climate* **24**: 159–182.

Serreze MC, Box JE, Barry RG, Walsh JE. 1993. Characteristics of Arctic synoptic activity, 1952–1989. *Meteorology and Atmospheric Physics* **51**: 147–164.

Serreze MC, Barrett AP, Stroeve JC, Kindig DN, Holland MM. 2009. The emergence of surface-based Arctic amplification. *The Cryosphere* **3**: 11–19.

Shimada K, Kamoshida T, Itoh M, Nishino S, Carmack E, McLaughlin F, Zimmerman S, Proshutinsky A. 2006. Pacific Ocean Inflow: influence on catastrophic reduction of sea ice cover in the Arctic Ocean. *Geophysical Research Letters* **33**: L08605. DOI: 10.1029/2005GL025624

Simmonds I, Keay K. 2009. Extraordinary September Arctic sea ice reductions and their relationships with storm behavior over 1979–2008. *Geophysical Research Letters* **36**: L19715. DOI: 10.1029/2009GL039810

Spekat A, Kreienkamp F, Enke W. 2010. An impact-oriented classification method for atmospheric patterns. *Physics and Chemistry of the Earth* **35**: 352–359.

Steele M, Ermold W, Zhang J. 2008. Arctic Ocean surface warming trends over the past 100 years. *Geophysical Research Letters* **35**: L02614. DOI: 10.1029/2007GL031651

Stroeve JC, Serreze MC, Fetterer F, Arbetter T, Meier W, Maslanik J, Knowles K. 2005. Tracking the Arctic's shrinking ice cover: another extreme September minimum in 2004. *Geophysical Research Letters* **32**: L04501. DOI: 10.1029/2004GL021810

Stroeve JC, Serreze MC, Holland MM, Kay JE, Maslanik J, Barrett AP. 2012. The Arctic's rapidly shrinking sea ice cover: a research synthesis. *Climatic Change* **110**: 1005–1027.

Thompson DWJ, Wallace JM. 1998. The Arctic Oscillation signature in the wintertime geopotential height and temperature fields. *Geophysical Research Letters* **25**: 1297–1300.

Vavrus SJ, Holland MM, Jahn A, Bailey DA, Blazey BA. 2012. Twenty-first-century Arctic climate change in CCSM4. *Journal of Climate* **25**: 2696–2710.

Wallace JM, Gutzler DS. 1981. Teleconnections in the geopotential height field during the Northern Hemisphere winter. *Monthly Weather Review* **109**: 784–812.

Wang J, Zhang J, Watanabe E, Ikeda M, Mizobata K, Walsh JE, Bai X, Wu B. 2009. Is the Dipole Anomaly a major driver to record lows in Arctic summer sea ice extent? *Geophysical Research Letters* **36**: L05706. DOI: 10.1029/2008GL036706

Wilks DS. 2011. *StatisticalMethods in the Atmospheric Sciences*, 3rd edn. Academic Press: Oxford, UK.

Woodgate RA, Weingartner T, Lindsay R. 2010. The 2007 Bering Strait oceanic heat flux and anomalous Arctic sea-ice retreat. *Geophysical Research Letters* **37**: L01602. DOI: 10.1029/2009GL041621

Yarnal B. 1993. *Synoptic Climatology in Environmental Analysis: A primer*. Belhaven Press: London, UK.

